



Microstructure and mechanical properties of 7A56 aluminum alloy after solution treatment

Feng-Bin Guo, Bao-Hong Zhu* , Long-Bing Jin, Guo-Jun Wang,
Hong-Wei Yan, Zhi-Hui Li, Yong-An Zhang, Bai-Qing Xiong

Received: 30 October 2016/Revised: 5 January 2017/Accepted: 7 November 2017
© The Nonferrous Metals Society of China and Springer-Verlag GmbH Germany, part of Springer Nature 2017

Abstract The effect of solution treatment on the microstructure and mechanical properties of a novel 7A56 aluminum alloy plate was investigated by optical microscopy (OM), scanning electron microscopy (SEM), transmission electron microscopy (TEM), X-ray diffraction (XRD), differential scanning calorimetry (DSC), conductivity, hardness and tensile tests. The results indicate that the coarse second phases in the hot-rolled plate mainly consist of AlZnMgCu quaternary phase and Al₇Cu₂Fe phase, and no Al₂CuMg phase is found. The amount of the second phases gradually reduces with the increase in temperature (450–480 °C) and time (1–8 h) during the solution treatment, and the soluble particles are completely dissolved into the matrix after solution treatment at 470 °C for 4 h, while the residual phases are mainly Fe-rich phase along the grain boundaries. The recrystallization fraction of the alloy gradually increases with the degree of solution treatment deepened. When the temperature exceeds 480 °C, over-burning takes place. The mechanical properties of samples treated at 470 °C for various times were tested. After the solution treated at 470 °C for 4 h, the quenching conductivity and peak-aged hardness of the alloy are 30.8%IACS and HV 204, respectively. The ultimate tensile strength and yield strength of the samples aged at 120 °C for 24 h are 661 and 588 MPa, respectively.

Keywords 7A56 aluminum alloy; Solution treatment; Aging treatment; Microstructure; Properties

1 Introduction

Al–Zn–Mg–Cu (7xxx) alloys are typical aging hardened materials, with the advantage of low density, high strength and good resistance to (stress corrosion cracking) SCC [1–5]. As a kind of crucial structural material, 7xxx alloys have been extensively used in commercial aircraft structures [6]. In order to acquire better properties, traditionally, the preparation process of 7xxx alloys mainly consist of casting, homogenization, pre-heating, rolling, solution and aging treatment. On the other hand, many researchers have focused on designing alloy composition for many years to obtain materials with excellent properties. [3, 7, 8]. With the rapid development of aerospace industry, increasing the solute content of the major alloying element, especially Zn and Mg, has become an important trend for 7xxx alloys [9]. 7A56 alloy which has high solute content was registered inland in 2015 and shows outstanding overall properties.

For 7xxx alloys, lots of coarse constituent particles can be found after the homogenization and rolling processing, due to the effect of slow cooling and deformation-induced precipitation (DIP) [10]. These constituent particles mainly contain Mg (Zn, Cu, Al)₂ (*T*-phase), Al₂CuMg (*S*-phase), Al₂Cu (*θ*-phase), Mg₂Si and Al₇Cu₂Fe. Some studies report that these second phases will badly deteriorate the properties of the alloy, such as intensity, fracture toughness and stress corrosion cracking resistance [11, 12]. Therefore, to obtain the preferable mechanical properties for 7xxx alloys, solution treatment will be carried out to dissolve most of coarse constituent particles. The aim of the present study is to investigate the optimal solution temper

F.-B. Guo, B.-H. Zhu*, L.-B. Jin, H.-W. Yan, Z.-H. Li,
Y.-A. Zhang, B.-Q. Xiong
State Key Laboratory of Nonferrous Metals and Processes,
General Research Institute for Nonferrous Metals, Beijing
100088, China
e-mail: zhuhb@grinm.com

G.-J. Wang
Northeast Light Alloy Co., Ltd., Harbin 150060, China

Table 1 Solution treatment temper for rolling plate of 7A56 alloy

Test Nos.	Solution treatment schedules
1	450 °C/1 h
2	460 °C/1 h
3	470 °C/1 h
4	480 °C/1 h
5	470 °C/2 h
6	470 °C/4 h
7	470 °C/6 h
8	470 °C/8 h

of the novel 7A56 alloy rolling plate to get the outstanding properties for the alloy.

2 Experimental

The material used in this study was a 40-mm-thick 7A56 alloy plate (9.2 Zn, 2.1 Mg, 1.8 Cu, 0.12 Zr, 0.09 Fe, 0.06 Si and the balance Al, in wt%) in hot-rolled condition. The samples were selected at quarter thickness of the plate, in order to ensure a maximum homogeneity of composition and grain structure. The solution temper for 7A56 alloy is detailed in Table 1.

Microstructures of the specimen were investigated by optical microscope (OM, Zeiss Axiovert 200), scanning electron microscope (SEM, JEOL JSM 7001F) and transmission electron microscope (TEM, JEOL 2010FX) [12–14]. Analysis of the composition of the second phases was carried out by energy-dispersive spectroscopy (EDS, VANTACE, DI4105). Graff segment reagent was used during the observation of OM. The melting temperature associated with the constituent particles in the specimen was measured by differential scanning calorimetric (DSC) conducted on NETZSCH STA 409 C/CD instrument with a heating rate of 10 K·min⁻¹ ranging from room temperature to 560 °C. The microstructural characterization was carried out by X-ray diffractometer (XRD, Rigaku D/Max 2500)

with a step of 0.5°. The conductivity of the quenching specimen was measured by WD-Z eddy current conductivity meter at room temperature. To ensure the validity of the results, six values were acquired. Specimens for hardness tests were prepared by mechanical grinding and polishing and then conducted on a Vickers hardness testing machine with a load of 50 N force and a loading duration of 10 s. For each specimen, at least ten indents were performed. The tensile specimens of 5 mm in gauge diameter and 25 mm in gauge length were cut along rolling direction in accordance with the ASTM standard E 517-00. The tensile test was measured by a WD 3100 test machine at a constant speed of 2 mm·min⁻¹.

3 Results and discussion

3.1 Observation of original microstructures

The optical microstructure of the 7A56 alloy rolling plate is shown in Fig. 1. It can be observed that a number of coarse constituent particles distribute along the rolling direction, with the dimensions of 3–50 μm. According to Refs. [10, 15], these constituent particles in the alloy were mainly produced in the process of homogenization and rolling deformation. EDS analysis reveals that these white second phases are mainly AlZnMgCu phases, which form during the dissolution of MgZn₂ phase, accompanied with Cu and Al atoms replacing Zn atoms [16]. And the gray particles are mainly Fe-rich phases, namely Al₇Cu₂Fe, which is nearly insoluble during the solution treatment in the 7xxx alloys. No Al₂CuMg phase could be found in the alloy. Most particles are expected to be dissolved into the matrix during the solution treatment. However, the high solution temperature inevitably leads to over-burning and recrystallization [17–19]. Therefore, it is necessary to optimize the solution treatment (Table 2).

Typical DSC thermogram is obtained for the rolling plates, and the result of DSC is shown in Fig. 2. There is an apparent endothermic peak around the temperature of

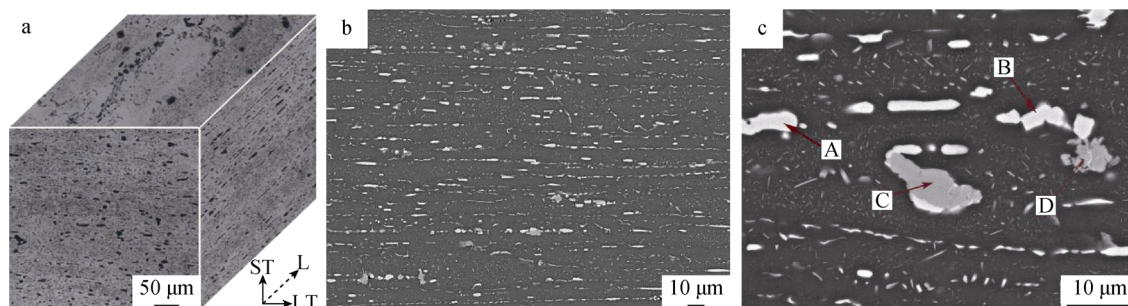
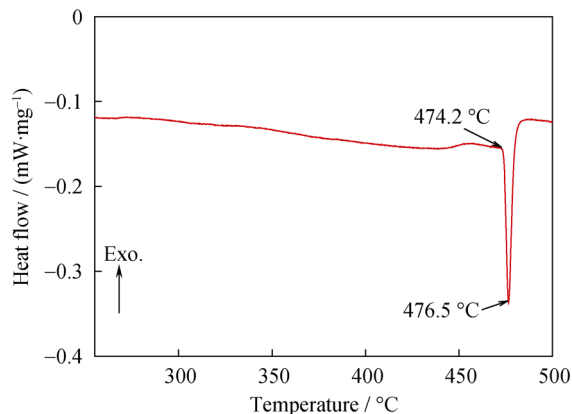


Fig. 1 Microstructure of as-rolled 7A56 alloy: **a** three-dimensional metallography of alloy (L, rolling direction; LT, long transverse; ST, short transverse); **b**, **c** photograph of alloy obtained by SEM

Table 2 EDS analysis of second phase in Fig. 1c (at%)

Label	Al	Zn	Mg	Cu	Fe
A	45.55	24.44	20.37	9.64	–
B	55.82	18.07	18.40	7.72	–
C	72.13	0.90	–	17.88	9.08
D	83.40	2.52	1.90	8.33	3.85

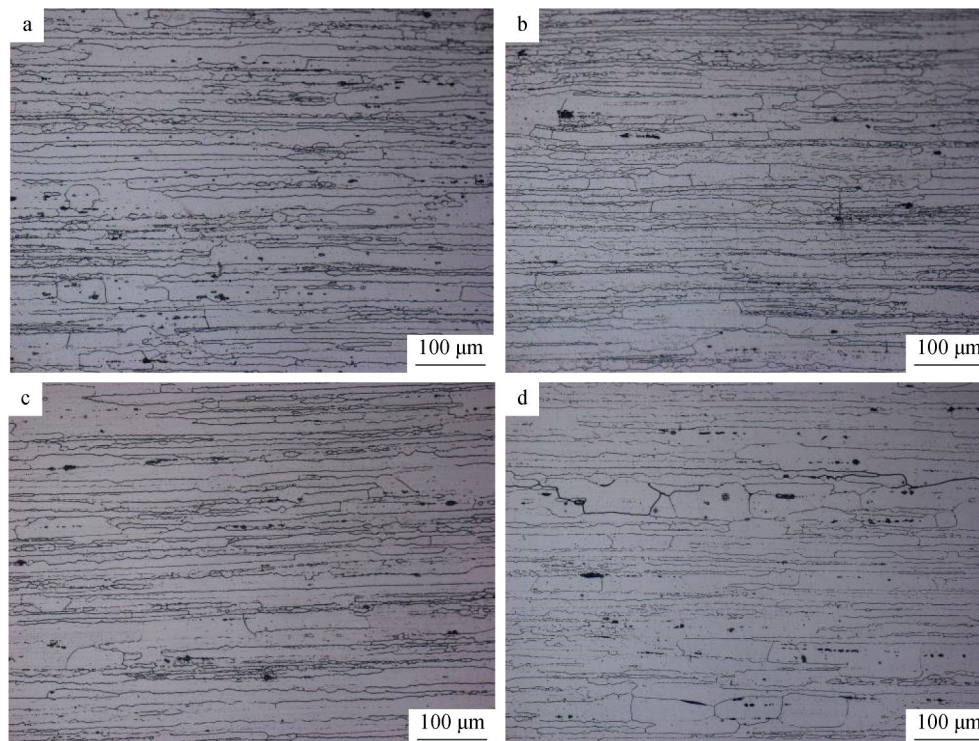
**Fig. 2** DSC test curve of 7A56 rolling plate

475 °C, and it is on behalf of the melting of AlZnMgCu phase [18, 20]. According to the analysis of data, the extrapolation initial temperature of this phase is 474.2 °C that the solution temperature should not exceed.

3.2 Dissolution of constituent particles and recrystallization

The typical optical microstructures of the samples, which were heated at different temperatures holding for 1 h followed by water quenching, are shown in Fig. 3. From the optical photographs, it is shown that the number density of the second-phase particles rapidly decreases after solution treatment, and with the holding temperature increasing from 450 to 470 °C, the number of remaining constituent particles decreases gradually. When the temperature exceeds 480 °C, apart from insoluble phases, the remaining constituent particles also could be seen, because of the over-burning of particles [20–22].

The dissolution process of the second phases was observed by SEM (Fig. 4). A number of uniformly constituent particles are dissolved into matrix after solution treatment. It could be obviously seen from the histogram in Fig. 5 that remaining constituent particles become less with the increase in the temperature. The area fraction of the second phases in the as-rolled plate is about 5.4%. After the

**Fig. 3** OM images of 7A56 alloy at different solution temperatures for 1 h: **a** 450 °C, **b** 460 °C, **c** 470 °C and **d** 480 °C

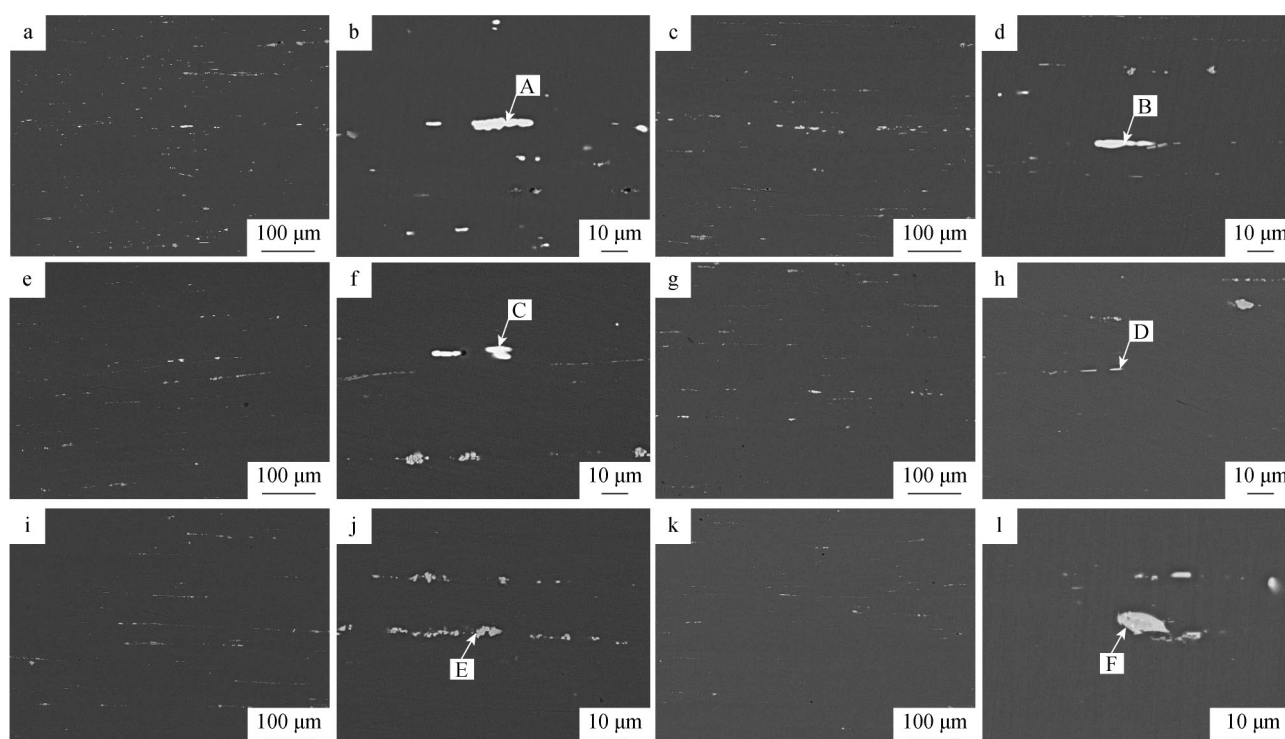


Fig. 4 SEM images of 7A56 alloy after solution treatment: **a, b** 450 °C, 1 h; **c, d** 460 °C, 1 h; **e, f** 470 °C, 1 h; **g, h** 470 °C, 3 h; **i, j** 470 °C, 4 h; **k, l** 480 °C, 1 h

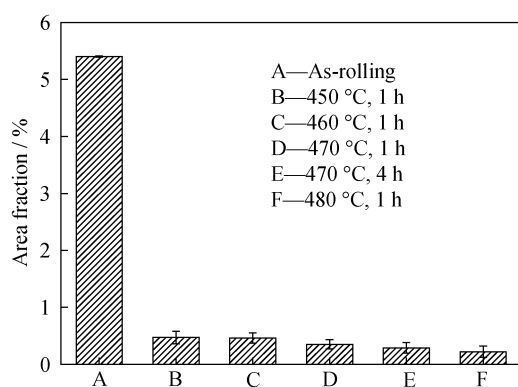


Fig. 5 Area fraction of the second-phase particles of 7A56 aluminum alloy

solution treatment at 450 °C for 1 h, the fraction reduces to 0.47%. With further elevating the solution temperature, the values decrease slowly.

XRD patterns of the samples treated at different temps (Fig. 6) also prove that the primary phases are α (Al) and MgZn_2 in the rolling plate. The peaks of $\text{Al}_7\text{Cu}_2\text{Fe}$ could be covered by the peaks of Al matrix and MgZn_2 . After solution treatment at all temps, the peak of MgZn_2 is not obvious, which means that there are few MgZn_2 phases in the treated samples.

In Table 3, the composition of the phases was analyzed by EDS. The AlZnMgCu phase, close to $\text{Mg}(\text{Zn}, \text{Cu}, \text{Al})_2$

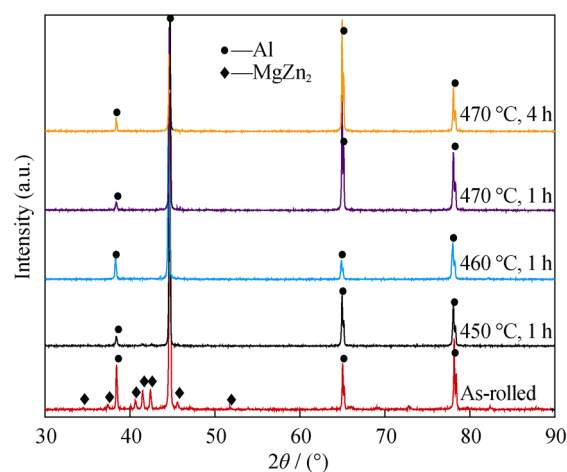


Fig. 6 XRD patterns of sample treated at different temps

phase in some positions, is observed in samples treated at 450, 460 and 470 °C for 1 h (marked as Arrows A, B, C in Fig. 4). Even after holding for 3 h at 470 °C, the similar composition phase (marked as Arrow D) can be found. But the size decreases gradually. Only Fe-rich phases are observed in the samples at 470 °C, 4 h (marked as Arrow E). That is to say, the second phases with low melting point are completely dissolved into the matrix [23]. When the temperature exceeds 480 °C, the eutectic phase takes place (marked as Arrow F). So, according to the observation of

Table 3 EDS analysis of constituent phases in Fig. 4 (at%)

Label	Al	Zn	Mg	Cu	Fe
A	31.3	25.76	25.85	17.08	–
B	23.58	26.66	29.59	20.17	–
C	29.12	22.51	32.62	15.74	–
D	32.61	21.82	30.24	15.33	–
E	75.09	1.26	0.73	14.44	8.48
F	55.85	17.83	15.53	10.80	–

microstructure, the optimal solution treatment temper of 7A56 alloy is 470 °C, 4 h.

The recrystallization of samples during various solution tempers is shown in Fig. 7. With the increase in the solution temperature and time, the degree of recrystallization of the sample deepens gradually. The area fraction of recrystallization for the hot-rolled sample is about 61.4% in Fig. 7a, and then, the value increases to 65.3% after solution treatment at 460 °C for 1 h (Fig. 7c). On the condition of the optimal solution treatment temper (Fig. 7d), the recrystallization area fraction of the sample is about 67.7%.

3.3 Quenching conductivity and hardness

Quenching conductivity and T6 aging hardness of 7A56 alloy were measured after solution treatment at 470 °C for different holding times in Fig. 8. The conductivity of the quenching samples decreases rapidly after solution treatment. Otherwise, there is no obvious change when extending the solution time. The minimum value of the quenching conductivity is 30.7%IACS when holding for

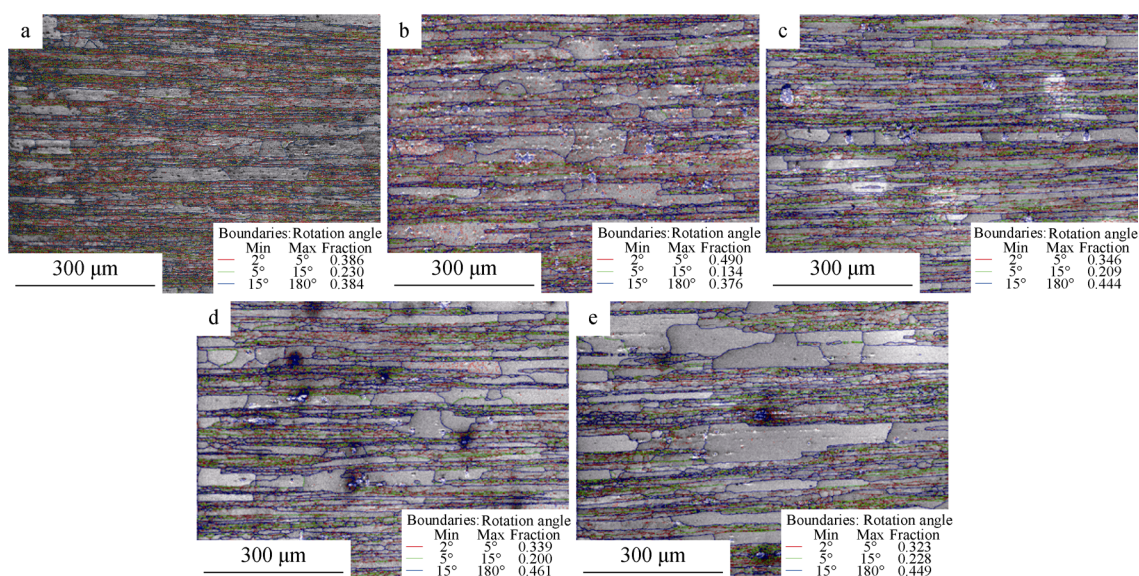
6 h. The variation trend of T6 aging hardness increases firstly and then decreases with the increase in holding time. The maximum value of aging hardness is HV 204 at 470 °C for 4 h. Considering the result of microstructure and properties of 7A56 alloy, the optimal solution temper should be 470 °C, 4 h.

3.4 Result of tensile test

According to the result of solution treatment for the quarter thickness of the plate, samples selected at the core of the plate were treated for aging treatment at 120 °C for different time. The corresponding curves of ultimate tensile strength, yield strength and elongation are presented in Fig. 9. As shown in Fig. 9a, b, the ultimate tensile strength (UTS) and yield strength (YS) increase rapidly during the early 6 h, followed by a gentler increase up to 60 h. In Fig. 9c, the elongation at break varies in the narrow range, about 10.2%–15.9%. The UTS and YS values of the sample after solution treatment are 570 and 388 MPa, respectively. The values increase to 648 and 558 MPa aged for 6 h, which increase by 14% and 44% for UTS and YS, respectively. By extending aging time, the increase in the values become slow, and when the aging time is 24 h, the UTS and YS values are 661 and 588 MPa, respectively. And then, the slow reduction of UTS is presented [24–26]. On the contrary, the YS of the alloy still increases.

3.5 Observation of precipitates

Figure 10a–c gives TEM images of the precipitates in the matrix and the grain boundary for the alloy specimen aged at 120 °C for 6, 24 and 40 h. All of the precipitates in the


Fig. 7 Backscattered electron SEM images of specimens: **a** hot-rolled; **b** 450 °C, 1 h; **c** 460 °C, 1 h; **d** 470 °C, 1 h; **e** 470 °C, 4 h

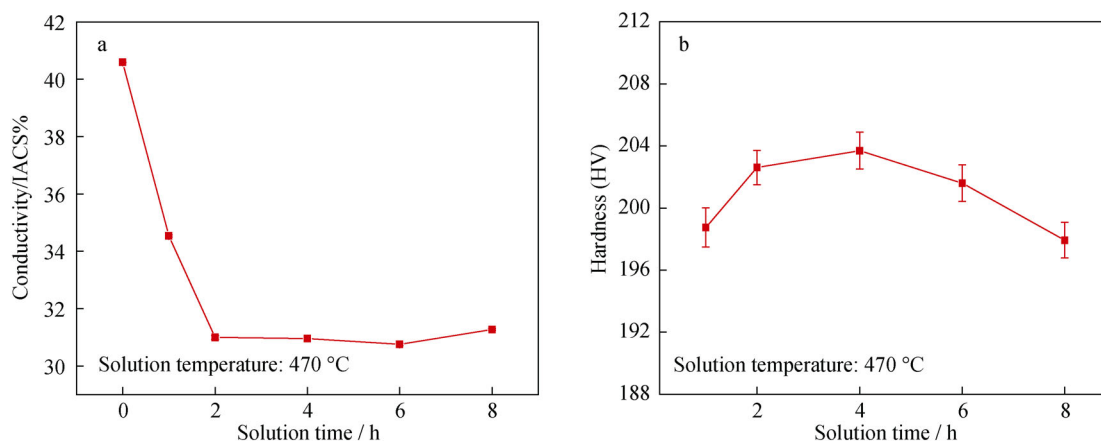


Fig. 8 **a** Quenching conductivity and **b** T6 aging hardness of 7A56 alloy for different time at 470 °C

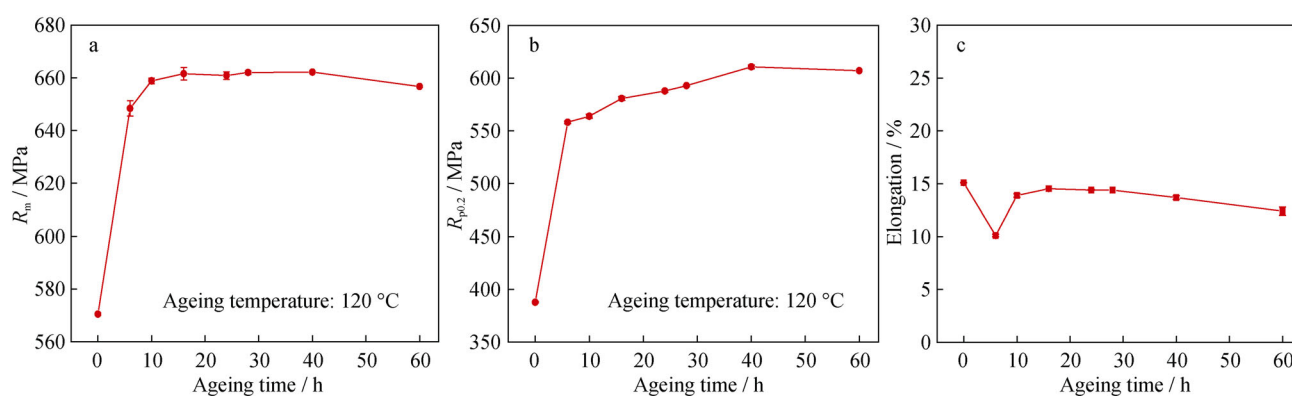


Fig. 9 **a** Ultimate tensile strength, **b** yield strength and **c** elongation of 7A56 alloy at 120 °C for different aging time

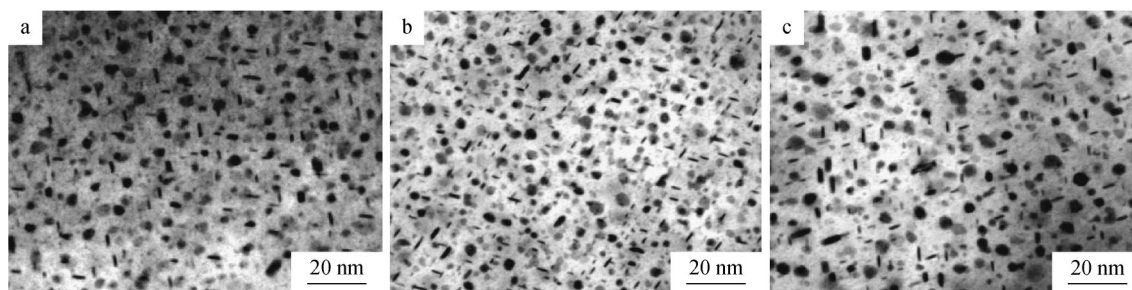


Fig. 10 TEM images of precipitates in matrix for samples aging at 120 °C for **a** 6 h, **b** 24 h and **c** 40 h

matrix are observed along the $\langle 110 \rangle_{Al}$ orientation. As shown in Fig. 10a, on the condition of aging treatment at 120 °C for 6 h, there are elliptical and elongated precipitates in the matrix with the size of 1–4 nm. Furthermore, the size of precipitates with shapes of ellipse and stick in matrix manifests a relatively homogeneous increment with the degree of aging treatment deepening in Fig. 10b, c.

4 Discussion

The aim of solution treatment is to dissolve the constituent particles into the matrix extremely to form supersaturated solid solution, so the nanophase will be precipitated mostly in the process of artificial aging to strengthen the properties of alloy [27–30]. At the same time, an undesirable result is that recrystallization occurs, which will deteriorate the properties of the alloy. For the novel 7A56 alloy, compared with the traditional Al–Zn–Mg–Cu alloy, high solute

concentration (about 13%) is the apparent characteristic, so it can get a higher intensity to meet the demand. For the as-rolled plate, the second phases formed in the deformation mainly contain AlZnMgCu and Fe-rich phases in the observation of original plates, without the traditional Al₂CuMg phase [4, 5, 8]. This agrees with studies on solution treatments that Al₂CuMg phase is formed at content of Cu + Mg \geq 3.6 wt% in 7xxx alloys containing around 6.0 wt% Zn [1]. The size of the second phase in the as-rolled is about 3–50 μ m, and the number is large. During the solution treatment, with the increase in temperature and time, the remaining soluble particles gradually become spheroidizing and the size becomes small. The AlZnMgCu phase disappears at 470 °C for 4 h. Only Fe-rich phase could be found. However, the degree of recrystallization of the sample deepens gradually. The area fraction of recrystallization for the hot-rolled sample is about 61.4%. The value increases to 67.7% after solution treatment at 470 °C for 4 h. When further elevating the temperature (\geq 480 °C), over-burning could occur. According to the result of tensile test, the UTS and YS increase rapidly during the early stage, followed by a gentler increase in the later stage, resulting from the growing of aging precipitates.

5 Conclusion

In the rolling plate of 7A56 alloy, it can be observed that a number of coarse constituent particles distribute along the rolling direction, mainly containing AlZnMgCu and Al₇Cu₂Fe phases. With the increase in the temperature and time during solution treatment, the remaining constituent particles would be less. At the same time, the recrystallization fraction of the sample increases gradually. The optimal solution temper should be 470 °C, 4 h. Conductivity and hardness of 7A56 alloy were measured. After solution treatment at 470 °C for 4 h, the conductivity of the quenching samples is about 30.8%IACS. The hardness of the specimen is HV 204 aged at 120 °C for 24 h. The result of tensile test shows that the peak-aged UTS and YS are 661 and 588 MPa, respectively.

Acknowledgements This work was financially supported by the National Key Research and Development Program of China (No. 2016YFB0300803), the National Natural Science Foundation of China (No. 51274046) and the National Key Basic Research Program (No. 2012CB619504).

References

- [1] Rometsch PA, Zhang Y, Knight S. Heat treatment of 7xxx series aluminium alloys-some recent developments. *Trans Nonferrous Met Soc China*. 2014;24(7):2003.
- [2] Xu DK, Birbilis N, Lashansky D, Rometsch PA, Muddle BC. Effect of solution treatment on the corrosion behaviour of aluminium alloy AA7150: optimisation for corrosion resistance. *Corros Sci*. 2011;53(1):217.
- [3] Chen ZY, Mo Y, Nie ZR. Effect of Zn content on the microstructure and properties of super-high strength Al–Zn–Mg–Cu alloys. *Metall Mater Trans A*. 2013;44(8):3910.
- [4] Peng GS, Chen KH, Chen SY, Fang HC. Evolution of the second phase particles during the heating-up process of solution treatment of Al–Zn–Mg–Cu alloy. *Mater Sci Eng A*. 2015;641(12):237.
- [5] Li PY, Xiong BQ, Zhang YA, Li ZH. Temperature variation and solution treatment of high strength AA7050. *Trans Nonferrous Met Soc China*. 2012;22(3):546.
- [6] Williams JC, Starke EA. Progress in structural materials for aerospace systems. *Acta Mater*. 2003;51(19):5775.
- [7] Liu JT, Zhang YA, Li XW, Li ZH, Xiong BQ, Zhang JS. Thermodynamic calculation of high zinc-containing Al–Zn–Mg–Cu alloy. *Trans Nonferrous Met Soc China*. 2014;24(5):1481.
- [8] Dumont D, Deschamps A, Bréchet Y. Characterization of precipitation microstructures in aluminum alloys 7040 and 7050 and their relationship to mechanical behavior. *Mater Sci Technol*. 2004;20(5):567.
- [9] Wen K, Fan YQ, Wang GJ, Jin LB, Li XW, Li ZH, Zhang YA, Xiong BQ. Aging behavior and precipitate characterization of a high Zn-containing Al–Zn–Mg–Cu alloy with various tempers. *Mater Des*. 2016;101(7):16.
- [10] Lang YJ, Zhou GX, Hou LG, Zhang JS, Zhuang LZ. Significantly enhanced the ductility of the fine-grained Al–Zn–Mg–Cu alloy by strain-induced precipitation. *Mater Des*. 2015;88(9):625.
- [11] Robson JD. Microstructural evolution in aluminum alloy 7050 during processing. *Mater Sci Eng A*. 2004;382(1–2):112.
- [12] Fang HC, Chen KH, Chen X, Chao H, Peng GS. Effect of Cr, Yb and Zr additions on localized corrosion of Al–Zn–Mg–Cu alloy. *Corros Sci*. 2009;51(12):2872.
- [13] Fan XG, Jiang DM, Meng QC. The microstructural evolution of an Al–Zn–Mg–Cu alloy during homogenization. *Mater Lett*. 2006;60(12):1475.
- [14] Xie F, Yan X, Ding L, Zhang F, Chen S. A study of microstructure and microsegregation of aluminum 7050 alloy. *Mater Sci Eng A*. 2003;355(1–2):144.
- [15] Li DF, Zhang DZ, Liu SD, Shan ZJ, Zhang XM, Wang Q, Han SQ. Dynamic recrystallization behavior of 7085 aluminum alloy during hot deformation. *Trans Nonferrous Met Soc China*. 2016;26(6):1491.
- [16] Xu DK, Rometsch PA, Birbilis N. Improved solution treatment for an as-rolled Al–Zn–Mg–Cu alloy. Part II. Microstructure and mechanical properties. *Mater. Sci. Eng A*. 2012;534(2):244.
- [17] Xu DK, Rometsch PA, Birbilis N. Improved solution treatment for an as-rolled Al–Zn–Mg–Cu alloy. Part I. Characterisation of constituent particles and overheating. *Mater. Sci. Eng A*. 2012;534(2):234.
- [18] Bolouri A, Shahmiri M, Cheshmeh ENH. Microstructural evolution during semisolid state strain induced melt activation process of aluminum 7075 alloy. *Trans Nonferrous Met Soc China*. 2010;20(9):1663.
- [19] Ralph B. *Light Alloys: From Traditional Alloys to Nanocrystals*. 4th ed. Oxford: Butterworth-Heinemann; 2006. 421.

- [20] Mazzer EM, Afonso CRM, Galano M. Microstructure evolution and mechanical properties of Al–Zn–Mg–Cu alloy reprocessed by spray-forming and heat treated at peak aged condition. *J Alloys Compd.* 2013;579(12):169.
- [21] Morere B, Ehrström JC, Gregson PJ. Microstructural effects on fracture toughness in AA7010 plate. *Metall Mater Trans A.* 2000;31(10):2503.
- [22] Zhang Y, Bettles C, Rometsch PA. Effect of recrystallisation on Al₃Zr dispersoid behaviour in thick plates of aluminium alloy AA7150. *J Mater Sci.* 2014;49(4):1709.
- [23] Starink MJ, Milkereit B, Zhang Y. Predicting the quench sensitivity of Al–Zn–Mg–Cu alloys: a model for linear cooling and strengthening. *Mater Des.* 2015;88(12):958.
- [24] Marlaud T, Malki B, Henon C, Deschamps A, Baroux B. Relationship between alloy composition, microstructure and exfoliation corrosion in Al–Zn–Mg–Cu alloys. *Corros Sci.* 2011; 53(10):3139.
- [25] Feng C, Liu ZY, Ning AL, Liu YB, Zeng SM. Retrogression and re-aging treatment of Al–9.99%Zn–1.72%Cu–2.5%Mg–0.13% Zr aluminum alloy. *Trans Nonferrous Met Soc China.* 2006; 16(5):1163.
- [26] Ryum N. The influence of a precipitate-free zone on the mechanical properties of an Al–Mg–Zn alloy. *Acta Metall.* 1968;16(3):327.
- [27] Zhang YH, Yang SC, Zhi JH. Microstructure evolution in cooling process of Al–Zn–Mg–Cu alloy and kinetics description. *Trans Nonferrous Met Soc China.* 2012;22(9):2087.
- [28] Yang W, Ji S, Zhang Q, Wang M. Investigation of mechanical and corrosion properties of an Al–Zn–Mg–Cu alloy under various ageing conditions and interface analysis of η' precipitate. *Mater Des.* 2015;85(15):752.
- [29] Gang S, Alfred C. Early-stage precipitation in Al–Zn–Mg–Cu alloy (7050). *Acta Mater.* 2004;52(15):4503.
- [30] Cai B, Adams BL, Nelson TW. Relation between precipitate-free zone width and grain boundary type in 7075-T7 Al alloy. *Acta Mater.* 2007;55(5):1543.